JOURNAL OF COMPUTATIONAL PHYSICS 99, 99–105 (1992)

An Algorithm for the Solution of Inverse Laplace Problems and Its Application in Flaw Identification in Materials

SHUVRA DAS AND AMBAR K. MITRA

Department of Engineering Science and Mechanics, Iowa State University, Ames, Iowa 50011

Received September 6, 1989; revised June 29, 1990

An algorithm for solving an inverse problem in steady state heat conduction is developed. In this problem, the location and shape of the inner boundary of a doubly connected domain is unknown. Instead, additional experimental data are provided at several points on the outer boundary. Through an iterative process, the unknown boundary is determined by minimizing a functional. Convergence properties of the algorithm are examined, and the stopping criterion for the iterative process is developed from numerical experiments in a simple case. The scheme is shown to perform well for the complex case of an L-shaped crack in a square domain. © 1992 Academic Press, Inc.

1. INTRODUCTION

In a direct problem, all the information necessary for the solution of the problem are given as boundary conditions. In inverse problems, sufficient boundary conditions are not provided. In some problems, additional information at some interior points may be known, and the conditions on the boundary are unknown. For other problems, the conditions on some portions of the boundary of the domain are over-specified while the shape of or condition on some other portions of the boundary is unknown. In this paper, a problem of the latter kind is examined. Such problems naturally occur in non-destructive testing where the shape of a flaw in the interior is determined by utilizing measurements on the boundary.

Consider the problem of steady state heat conduction in a two-dimensional domain D shown in Fig. 1. Some parts ($S1_n$) of the boundary of the domain are insulated, and the rest ($S1_d$) is exposed to a steady temperature distribution. The temperature in this steady heat conduction problem satisfies the Laplace equation. Also consider that the temperature at $S1_n$ is obtained experimentally at several selected points. If the domain is punctured or contains a flaw ($S2$) as shown in Fig. 2, the measured temperature will be different from that for an unpunctured clean domain. Conversely, this difference in temperature indicates the presence of the flaw. Further, one can use the specified temperature and flux conditions on $S1_n + S1_d$, and the additional experimental information, and attempt to determine the location and shape of the flaw. The uniqueness of the solution to the problem of this nature has been discussed by Ramm [7].

In a recent review, Tanaka [10] has outlined several algorithms that have been employed in the solution of various kinds of inverse problems involving potential fields, elastostatic fields, and scalar wave fields. Murai and Kagawa [6] employed the influence coefficient approach in which the influence coefficient matrix is obtained by calculating the effect of shifting one node on all other nodes. In an iterative process, the nodes on the guessed boundary are shifted until the desired effect on a known boundary is

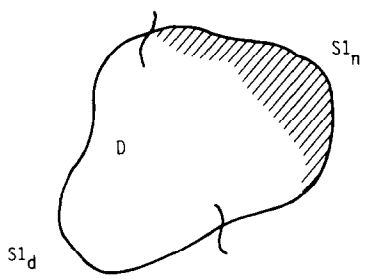

FIG. 1. Domain without flaw.

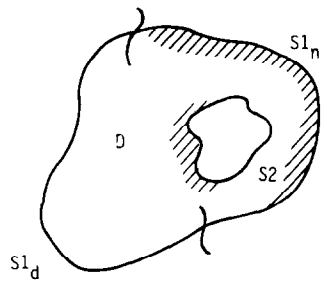

FIG. 2. Domain with a real flaw.

0021-9991/92 $3.00

achieved. Yoshikawa *et al.* [11] obtained the solidification line in a blast furnace by minimizing a functional which is formed by squaring and adding the difference between experimental and computed temperatures. However, the iterative method converges only when it is coupled with a regression analysis. Tanaka and Masuda [9] used a Taylor series expansion of the boundary integral equation to obtain the unknown boundary by distorting a guessed boundary in an iterative process. This method requires additional care in evaluating singular integrals which appear due to the differentiations in the Taylor expansion.

In the present paper, an algorithm is presented in which a functional, which is substantially different from that used by Yoshikawa *et al.* [11], is minimized in an iterative process to arrive at the unknown boundary by distorting a guessed boundary. The method converges without any difficulty, and the procedure does not involve evaluation of singular integrals. The algorithm is employed in solving three example problems. For one of the examples, the convergence pattern and its dependence on the number of experimental data points are demonstrated and the relationship between the minimum value of the functional and the accuracy of the solution is examined.

The present work is similar to some recent research on optimal shape design. In such design problems, a functional is minimized in order to arrive at the optimum geometry. Mota Soares *et al.* [4] and Mota Soares and Choi [5] have used the boundary integral equations in conjunction with non-linear programming technique to determine the optimal shape of a shaft. In these works, the set of nodal coordinates on the required geometry were treated as the degrees of freedom.

In the present work, the emphasis is on the algorithm rather than the use of such technique in a practical situation. Further work on the applicability is anticipated.

2. THE PROBLEM

Consider the problem of steady state heat conduction through a two dimensional domain D whose outer boundary is $S1$ (Fig. 1). Certain temperature distribution is maintained on a portion of the outer boundary ($S1_d$), and the rest of the boundary ($S1_n$) is insulated.

The temperature distribution on the insulated boundary, $S1_n$, can be obtained numerically by solving the boundary value problem for the Laplace equation, and also experimentally by attaching temperature recording probes to the insulated boundary. Ideally, the experimentally recorded and the numerically obtained values should match within certain acceptable limits. But, this may not always happen. There could be a flaw at an unknown location, and of unknown shape and size inside the domain D. Being unaware of the existence of the flaw, it will not be included in the numerical calculation. Yet it will affect the experimental recordings. As a result, the two values, numerical and experimental, of the temperature would not match. This matching procedure can thus be used as a test for establishing the existence of flaws. Such a procedure will be applicable in the laboratory only when the actual disturbances caused by the flaw are not masked by the errors in computation and measurements. If the numerical and experimental temperature values match, then there is no flaw. In the present work we have assumed that there could only be one flaw in the domain D.

Once it is clear from the test that the flaw exists, the domain of the problem changes from a simply connected to a doubly connected one with $S2$ (Fig. 2), the flaw, as its inner boundary. Although the location and the geometry of the flaw are unknown, the boundary condition on $S2$ is known to be the homogeneous Neumann condition. This corresponds to the physical situation of a flaw with very small conductivity. Our aim is to determine $S2$ from the measured temperature data on $S1_n$. The scheme for solving this inverse problem is described in the following section.

3. THE TECHNIQUE

The differential equation which governs steady state heat conduction is

$$\nabla^2 T = 0, \qquad \text{in} \quad D, \tag{1}$$

and the boundary conditions are

$$\begin{aligned} T(q) &= T_0(q), && q \in S1_d, \\ \frac{\partial T(q)}{\partial n_q} &= 0, && q \in S1_n, \\ \frac{\partial T(q)}{\partial n_q} &= 0, && q \in S2, \end{aligned} \tag{2}$$

where n_q is the outward normal drawn at q. The differential equation can be converted into the boundary integral equation [1],

$$\eta T(p) = \int_{S1_d + S1_n + S2} (G'T(q) - GT'(q))\, dS, \tag{3}$$

which connects the temperature at any point p with the boundary data. The ($'$) denotes the derivative $\partial/\partial n_q$ and the points p and q are known as the source and the field points, respectively. The coefficient η is given as

$$\begin{aligned} \eta &= 0, && \text{if} \quad p \text{ lies outside } D + S1_d + S1_n + S2 \\ &= 2\pi, && \text{if} \quad p \text{ lies inside the domain } D \\ &= \alpha, && \text{if} \quad p \text{ lies on } S1_d + S1_n + S2, \end{aligned} \tag{4}$$

where α is the included angle between two adjacent tangents at p. The function G is the fundamental solution of Laplace equation in two dimensions, and is known to be $\ln|p-q|$. Inserting the boundary conditions from Eq. (2), Eq. (3) simplifies to

$$\eta T(p) = \int_{S1_d} (G'T_0(q) - GT'(q))\, dS + \int_{S1_n} G'T(q)\, dS + \int_{S2} G'T(q)\, dS. \tag{5}$$

The first step of the scheme is to assume a flaw boundary $S3$ (Fig. 3). Ignoring the real flaw for the time being, the boundary integral equation, for the domain bounded externally by $S1_d + S1_n$ and internally by $S3$, is

$$\eta T(p) = \int_{S1_d} (G'T_0(q) - GT'(q))\, dS + \int_{S1_n} G'T(q)\, dS + \int_{S3} G'T(q)\, dS, \tag{6}$$

in which the following boundary conditions have been applied:

$$\begin{aligned} T(q) &= T_0(q), && q \in S1_d \\ \frac{\partial T(q)}{\partial n_q} &= 0, && q \in S1_n \\ \frac{\partial T(q)}{\partial n_q} &= 0, && q \in S3. \end{aligned} \tag{7}$$

We now plan to develop an algorithm which would distort the assumed flaw $S3$ until $S2 = S3$. However, at the beginning of the procedure, $S2 \neq S3$, and the temperature (T) and the flux (T') values appearing in Eq. (5) and Eq. (6) are different. Hence, for clarity, we add a subscript 2 to T and T' when the inner boundary is $S2$, and use subscript 3 when the inner boundary is $S3$, and rewrite equations (5) and (6) as

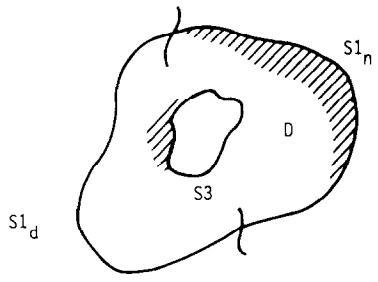

FIG. 3. Domain with the guessed flaw.

$$\eta T_2(p) - \int_{S1_n} G'T_2(q)\, dS = \int_{S1_d} (G'T_0(q) - GT_2'(q))\, dS + \int_{S2} G'T_2(q)\, dS \tag{8}$$

$$\eta T_3(p) - \int_{S1_n} G'T_3(q)\, dS = \int_{S1_d} (G'T_0(q) - GT_3'(q))\, dS + \int_{S3} G'T_3(q)\, dS. \tag{9}$$

If one substitutes $S2 = S3$, $T_2(q) = T_3(q)$, and $T_2'(q) = T_3'(q)$ in all the terms on the right-hand side of Eq. (8), this equation will not be satisfied any more. Denoting the error in Eq. (8) after such a substitution by δ, we can write

$$\eta T_2(p) - \int_{S1_n} G'T_2(q)\, dS = \int_{S1_d} (G'T_0(q) - GT_3'(q))\, dS + \int_{S3} G'T_3(q)\, dS + \delta(p). \tag{10}$$

Now subtracting Eq. (9) from (10) we obtain

$$\eta(T_2(p) - T_3(p)) + \int_{S1_n} (G'T_3(q))\, dS - \int_{S1_n} (G'T_2(q))\, dS = \delta(p). \tag{11}$$

The temperature $T_2(p)$ is assumed to be known from experiments for the real flaw at N number of selected points, $p_1, p_2, ..., p_N$ on $S1_n$. Equation (11) for one such selected point p_n is

$$\eta(T_2(p_n) - T_3(p_n)) + \int_{S1_n} (G'T_3(q))\, dS - \int_{S1_n} (G'T_2(q))\, dS = \delta(p_n) = \delta_n. \tag{12}$$

Now, each term of Eq. (12) will be examined:

Term 1. $T_2(p_n)$ is obtained from experiments; and $T_3(p_n)$ is obtained from numerical solution and can be updated as the minimization proceeds.

Term 2. Temperature $T_3(q)$ at $S1_n$ can be obtained numerically for the guessed flaw boundary $S3$ and updated as the minimization proceeds.

Term 3. The experimentally measured data, $T_2(p_n)$, on the boundary $S1_n$ is interpolated to obtain $T_2(q)$.

Altogether, one can evaluate N quantities $[\delta_n, n = 1, 2, 3, ..., N]$ for the N number of selected points $p = p_1, p_2, ..., p_N$. Then one can form the functional

$$F = \sum_{n=1}^{N} \delta_n^2$$

and minimize it. During the minimization process, the quantities $S3$ and $T_3(q)$ are modified, and at the conclusion of the process $S3$ converges to $S2$. The formulation of the problem as a minimization procedure has enabled us to use a commercially available package for the solution. The details of the algorithm for updating the unknowns at the end of each cycle is presented in the following section.

4. THE ITERATIVE PROCESS

In all the problems considered here, the outer boundary is a square which is divided into eight elements. On each element, the temperature and flux are assumed to be linear.

The real unknown flaw, $S2$, could be of any general shape. A very precise description of an odd-shaped flaw by using only straight elements, which we plan to use for simplicity, will require very fine discretization. The coordinates of the end points of such elements will then be the ultimate unknowns in the problem. For each additional element, the size of the problem is increased by two unknowns which are the coordinates of one end point of the added element. Soon, the procedure becomes computationally lengthy and economically unsound. As a remedy, in the present scheme, all flaws are assumed to be elliptic.

There are two reasons behind such an assumption. First, in nondestructive evaluation, the location of the flaw and an estimate of the linear dimensions of the flaw is usually adequate. The precise shape of the flaw is not required. Second, it has been found by the authors and other researchers [4, 5] that the nodal coordinates are not the suitable variables. Mota Soares and Choi [5] have observed that when the nodal variables are used, too much freedom is given to the problem which gives rise to kinks on the boundary $S2$. Authors' preliminary calculations support this observation. During the iterative refinement of $S2$, the nodal coordinates can move in such a fashion that the boundary $S2$ wraps around itself and finally lead to unrealistic solution. In order to avoid such unrealistic solutions, Saigal and Kane [8], while studying a shape optimization system for aircraft components, restricted the movement of the nodal points by retaining them on B-splines.

The assumption that all flaws are elliptic reduces the degree of freedom, and thereby reduces the computation time. The possibility of unrealistic solutions is also avoided by restraining the movement of the nodal points. Further, the elliptic shape covers a wide range of shapes from circular holes to straight cracks. In addition, the assumption regarding elliptic flaws is found to work well for a flaw which is very much different from an ellipse (see Example 3). The algorithm yields excellent estimates for the location, area, and linear dimensions of the flaw.

The ellipse is discretized by eight elements. Instead of considering the coordinates of the end points of these elements as the unknowns (degrees of freedom = 16), the semi-major axis (a), the semi-minor axis (b), location of the center (x_c, y_c), and the angular orientation (ϕ) of the major axis with a fixed global direction are considered as the ultimate unknowns of the problem (degrees of freedom = 5). Ideally one must obtain $T_2(p_n)$ from experiments, however, for want of any experimental data, a Laplace solver, based on boundary integral equation method, was used to compute $T_2(p_n)$. This Laplace solver is also used in conjunction with the minimization routine in the following calculations.

At the beginning of the iteration process, an initial guess for $S3$ is chosen, and for this guessed flaw, the $T_3(q)$ is calculated by using the Laplace solver. A subroutine named as FCN then calculates the functional using the description of $S3$ (as given by the 5 degrees of freedom), $T_3(q)$, and $T_2(p_n)$. For the minimization, the IMSL subroutine called UNLSF has been used. This subroutine uses the functional calculated by FCN, and updates the 5 degrees of freedom that define $S3$. The subroutine UNLSF is based on the Levenberg–Marquardt [2, 3] algorithm. The routine UNLSF calculates the derivatives of the functional internally, and the user need not furnish expressions for these. The updated $S3$ is then used by the Laplace solver to update $T_3(q)$. The functional is then calculated by FCN, and the process continues till convergence. During each cycle of the iterative minimization process, the Laplace solver updates $T_3(q)$, and UNLSF updates $S3$. This division of duties is computationally more efficient. If one forces UNLSF to update all the unknowns, e.g., $S3$ and $T_3(q)$, then it would have to deal with too many variables and would slow down the convergence significantly. Further, solution for too many variables would require a large value of N and would entail an unreasonable experimental effort to obtain $T_2(p_n)$ at too many points. Although the method, outlined above, involves repeated solution of discretized integral equations, the computational cost is acceptable since the convergence is fast.

5. EXAMPLES

In this section the results for three example problems are presented. Through these examples, the convergence

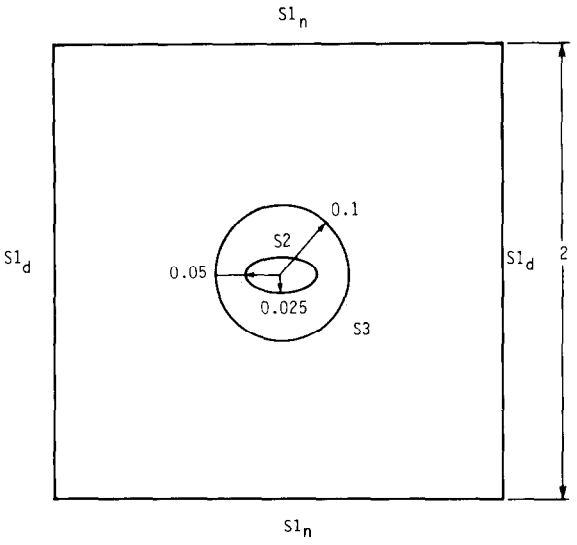

FIG. 4. Geometry of Example 1.

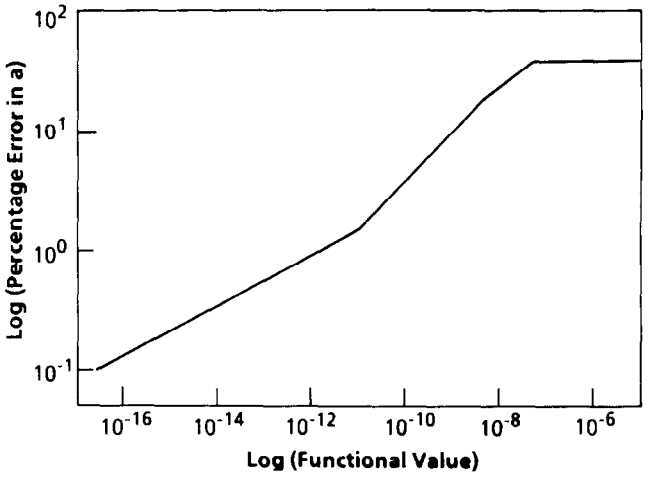

FIG. 5. Relationship between the value of the functional and the error in the value of the semi-major axis.

properties of the scheme, and its performance for a non-elliptic flaw will be demonstrated. In all the examples, the outer boundary is a 2×2 square. The origin of the cartesian axis system is located at the center of the square, with x-axis horizontal, and y-axis vertical. The vertical sides of the square are held at temperatures of 400 and 50°. The other two sides are insulated. Computations in all the cases begin with a guessed flaw in the shape of a circle of radius 0.1 which is located symmetrically at the center of the domain.

5.1. EXAMPLE 1. In this example the actual flaw is elliptic, with $a = 0.05$, $b = 0.025$, $x_c = y_c = 0$, and $\phi = 0$. The geometry of the problem is shown in Fig. 4. The problem is solved for $N = 8$, 10, and 12. Recalling that N is the number of probes used for the experimental measurements, half of these probes are placed on the top and half on the bottom surface of the square domain. The performance of the algorithm for these values of N is shown in Table I. For all values of N, the minimization process was continued until the value of the functional reduces to the order of 3×10^{-19}. The relative errors in semi-major and semi-minor axes at the "convergence" (which corresponds to $F = O(10^{-19})$ for the present discussion) are shown in columns 4 and 5 of Table I. The data show that the number of iterations is independent of the number of probes. Further, N has no influence on the accuracy of the solution. However, one should not choose $N < 5$, because that would lead to an underdetermined problem, and the results are found to be markedly inferior. Next we would examine, how far one should continue the minimization process. We begin with the notion that the relative errors in each of the five unknowns at any stage of iteration depends on the value of the functional at that stage. The relationship between the value of the functional and the percent error in the value of semi-major axis of the ellipse is shown in Fig. 5. This diagram shows that at the initial stages, the value of the semi-major axis improves very slowly. In the intermediate stage, the convergence is rapid, and in the final stage, any further reduction in the value of the functional causes insignificant improvement in accuracy. However, Fig. 5 shows that the value 10^{-12} of the functional corresponds to

TABLE I

N	Functional	I	Percent error in a	Percent error in b
8	2.623 E-19	81	0.1	0.04
10	2.623 E-19	83	0.1	0.04
12	2.623 E-19	83	0.1	0.04

Note. I = number of iterations; N = number of probes on the boundary.

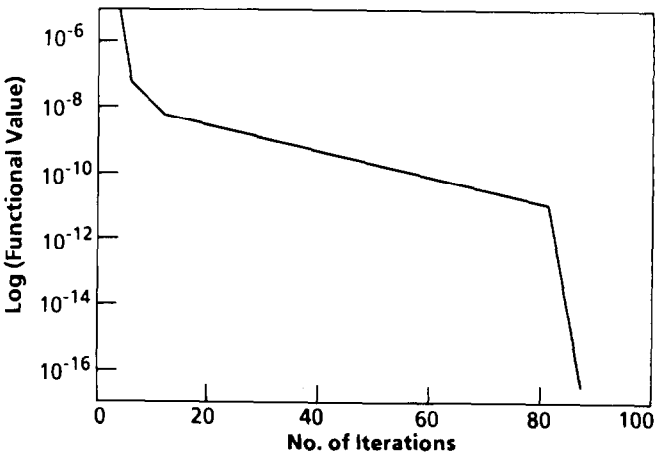

FIG. 6. Variation of the value of the functional with the number of iterations.

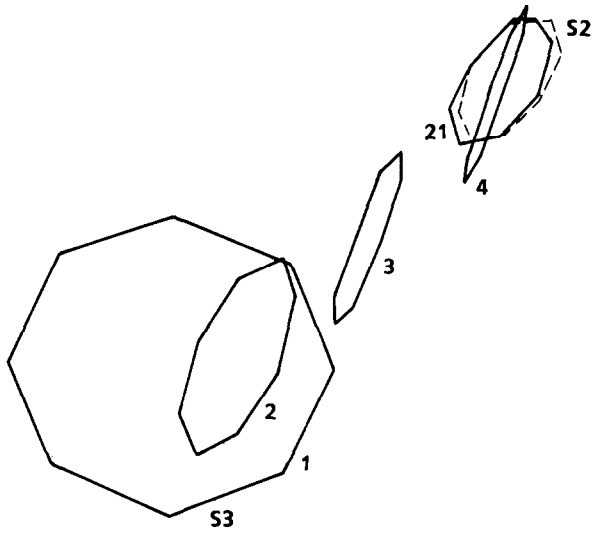

FIG. 7. Predicted flaw at different stages of iteration for Example 2.

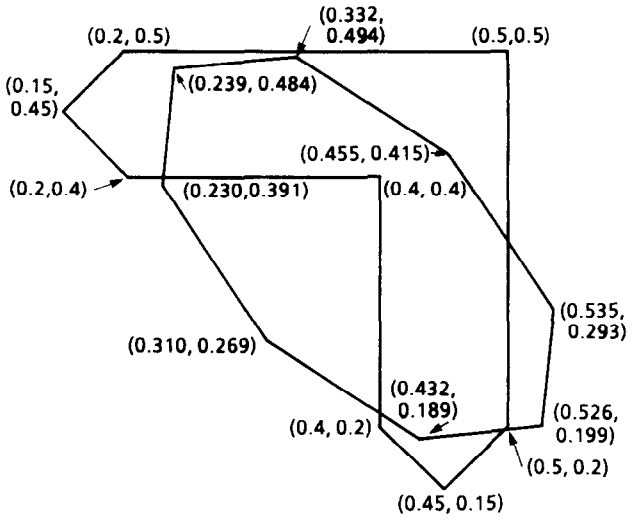

FIG. 9. Blow up of predicted and actual flaws of Example 3.

roughly 1% error, and for the following examples the iteration was stopped when the minimization reaches this stage. In Fig. 6, the number of iterations necessary for attaining different levels of accuracy is shown.

5.2. EXAMPLE 2. In this example, the flaw is still elliptic but is now located off-center. The variables defining the flaw are $a = 0.05$, $b = 0.025$, $x_c = y_c = 0.2$, $\phi = 45°$. In Fig. 7, the dynamics of the iterative process is simulated by showing the shape of the octagon (discretized ellipse) at various stages of iteration. This diagram shows that after 21 iterations the predicted flaw closely resembles the actual flaw. However, the computer program arrives exactly at the real flaw only after 80 iterations. The value of N was chosen to be 8, and the execution was stopped when the value of the functional reached 10^{-12}.

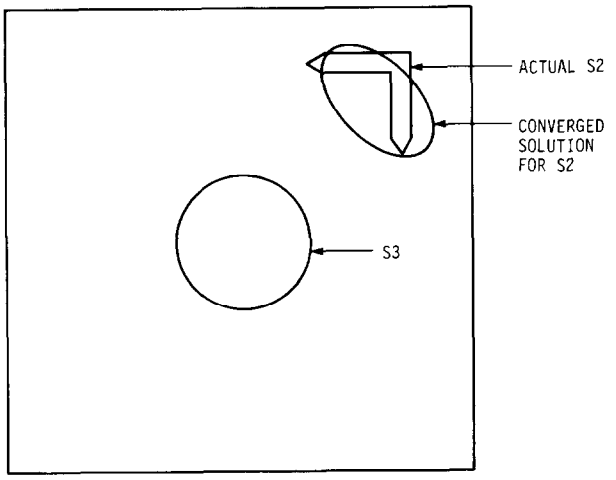

FIG. 8. Geometry of Example 3.

5.3. EXAMPLE 3. In order to demonstrate the superior performance of the scheme for non-elliptic flaws, it was employed in detecting an L-shaped crack shown schematically in Fig. 8 which is not drawn to scale. The crack width is 0.1 and the length of the arms is 0.3. Once again, the number of probes used was 8. The coordinates of the corners of the crack and converged octagon are shown as a blow up in Fig. 9. The algorithm identifies the location of the crack very well and provides an excellent estimate of the linear dimensions of the crack. The area of the crack is 0.055, and the area of the octagon is 0.06. The centroid of the crack is located at (0.383, 0.383) and the centroid of the octagon at (0.383, 0.342). The number of iterations required for this solution is 29. The value of the functional at convergence is of the order of 10^{-9}. This is understandable since the elliptic shape cannot exactly model an L-shaped flaw.

6. DISCUSSION

The performance of the simple algorithm based on the minimization of a functional was found to be excellent in several test cases. In this algorithm, the flaw is assumed to be an ellipse which is uniquely defined by five quantities. This assumption would enable one to extend the method to three dimensions, where the number of variables will be nine. Numerical experimentation for a simple case provided good guidelines for fixing the number of experimental data points and established the criterion for stopping the iterative process. Employment of these guidelines produced an excellent solution for a non-elliptic flaw. The algorithm developed here for the temperature field could presumably to extended to elastostatics, scattering, and electromagnetic fields.

An attempt has been made to evaluate the applicability of this method for real experimental data which may have measurement errors. Although the observations are inconclusive, the algorithm does not tolerate experimental errors which mask the effect of the flaw. For practical application, this deficiency should be eliminated. Research in that direction is currently in progress, and the results will be reported elsewhere.

REFERENCES

1. G. Fairweather, F. J. Rizzo, D. J. Shippy, and Y. S. Wu, *J. Comput. Phys.* **31** (1979).
2. K. Levenberg, *Q. Appl. Math.* **2** (1944).
3. D. W. Marquardt, *J. Soc. Ind. Appl. Math.* **2**, 11 (1963).
4. C. A. Mota Soares, R. P. Leal, and K. K. Choi, *Computer Aided Optimal Design: Structural and Mechanical Systems*, edited by C. A. Mota Soares (Springer-Verlag, Berlin, 1986), p. 605.
5. C. A. Mota Soares and K. K. Choi, *The Optimum Shape*, edited by J. A. Bennett and M. E. Botkin (Plenum, New York, 1986), p. 199.
6. T. Murai and Y. Kagawa, *Int. J. Numer. Methods Eng.* **23**, 35 (1987).
7. A. G. Ramm, *Inverse Probl.* **2**, L19 (1986).
8. S. Saigel and J. H. Kane, private communication.
9. M. Tanaka and Y. Masuda, *Eng. Anal.* **3**, 138 (1986).
10. M. Tanaka, in *Boundary Elements X, Southampton, England, 1988*, edited by C. A. Brebbia (Springer-Verlag, Berlin, 1988), p. 567.
11. F. Yoshikawa, S. Nigo, S. Kiyohara, S. Taguchi, H. Takahashi, and M. Ichikawa, *Iron Steel* **73**, 2068 (1987).